Luminescence Properties Of Dy^{3+} Doped $Gd_2(WO_4)_3$ Phosphor Prepared by Hydrothermal Method

Zhengyang Zhang†,*, Jinkai Li †, Wenzhi Wang, Guangbin Duan, Weilin Zhao, Zongming Liu*

School of Materials Science and Engineering, University of Jinan, Jinan, Shandong 250022, China

* Corresponding author:

† The two authors contributed equally to this paper.

E-mail: mse_zhangzy@163.com; ost_liuzm@ujn.edu.cn

Abstract. The Dy^{3+} doped $Gd_2(WO_4)_3$ phosphors have been successfully obtained through calcining the precursor prepared via hydrothermal method at 900℃. The structure, morphology and luminescent properties of the resultant products were characterized by X-ray diffraction (XRD), field emission scanning electron microscopy (FE-SEM), photoluminescence excitation/photo-luminescence spectroscopy (PLE/PL), and fluorescence decay analysis. The $(Gd_{1-x}Dy_x)_2(WO_4)_3$ (x=0.01-0.10) solid solutions, exhibit strong yellow luminescence at 575 nm (the $^4F_{9/2}\rightarrow{}^6H_{13/2}$ electric dipole transition of Dy^{3+}) optimal UV excitation into the $^6H_{15/2}\rightarrow{}^4H_{11/2}$ of Dy^{3+} at ~452 nm. The quenching concentration was determined to be ~7at.%, and the quenching was due to the exchange reaction between Dy^{3+}. The emission intensity decreased monotonically with the used temperature increasing while the fluorescence lifetime (0.5±0.05 ms) does not alter appreciably. All the $(Gd_{1-x}Dy_x)_2(WO_4)_3$ phosphors have similar CIE chromaticity coordinates and color temperatures of (~0.43±0.02, ~0.47±0.02) and ~3550 K respectively, but the lifetime for 575 nm emission decreased with the Dy^{3+} increasing ascribed to the energy transfer between Dy^{3+}. The $Gd_2(WO_4)_3$:Dy^{3+} yellow phosphors are expected to be widely used in white light LED and display areas.

1. Introduction

Tungstate $Ln_2(WO_4)_3$ (Ln=rare earth) is one of the most classical inorganic luminescent materials which could be widely used in lighting and display areas due to its good physical and chemical properties [1]. $Gd_2(WO_4)_3$ is a bottom centered monoclinic structure [2]. Ln^{3+} ion in $Ln_2(WO_4)_3$ could be replaced by various activators and exhibit colorful emission. Zhang et al. prepared Eu^{3+} doped Gd_2WO_6 and $Gd_2(WO_4)_3$ nanophosphors via co-precipitation method [3]; Liu et al. prepared Eu^{3+} doped $Gd_2(WO_4)_3$ and studied energy transfer [4]; Zeng et al. prepared Eu^{3+}/Tb^{3+} doped $Gd_2(WO_4)_3$ nanophosphors by hydrothermal method [5].

Dy^{3+} doped $Gd_2(WO_4)_3$ system was chosen in the present work based on the following three reasons: (1) WO_4^{2-} ion itself can effectively absorb the spectrum of blue violet LED emission, and transfer to the rare earth ions doped in tungstate matrix [6]. (2) The characteristic emission peak of Gd^{3+} at 275 nm overlapped with the excitation band of many activator ions, and thus the Gd^{3+} could be

usually served as a kind of effective sensitizer [7-8]. The Dy^{3+} emission in $Gd_2(WO_4)_3$ system could be further improved through the $Gd^{3+}\rightarrow Dy^{3+}$ energy transfer. (3) The Dy^{3+} mainly consisted two emission bands at 480 nm (blue emission) and 575 nm (yellow emission) corresponding to the $^4F_{9/2}\rightarrow{}^6H^{15/2}$ and $^4F_{9/2}\rightarrow{}^6H_{13/2}$ transitions of Dy^{3+}, respectively. The Dy^{3+} emission was effected significantly by the matrix material, and the emission color of Dy^{3+} could be adjusted by modulation the coordination environment [9-11]. This makes Dy^{3+} doped phosphors possess multi-functional performance, and thus have been extensively studied in the recent years.

Rare earth ions doped $Gd_2(WO_4)_3$ phosphors usually were synthesized, however, there are few reports about hydrothermal synthesis which can control the morphology and size of resultant products easily. In this work, we synthesized $Gd_2(WO_4)_3$:Dy^{3+} nanoscale phosphor by hydrothermal method. The resultant products were systematically studied using the combined techniques of XRD, FE-SEM, PLE/PL spectroscopy and fluorescence decay analysis. In the following, we report the synthesis, phase evolution, and the optical properties of $Gd_2(WO_4)_3$:Dy^{3+} samples in detail.

2. Experiment Section

2.1. Materials

The started chemicals required in this work mainly include gadolinium oxide (Gd_2O_3, 99.99%, Huizhou Ruier Rare Chemical Hi-Tech Co. Ltd., Huizhou, China), dysprosium oxide (Dy_2O_3, 99.99%, Huizhou Ruier Rare Chemical Hi-Tech Co. Ltd., Huizhou, China), sodium tungstate dihydrate ($Na_2WO_4{\cdot}2H_2O$, 99.5%, Sinopharm Chemical Reagent Co. Ltd., Shanghai, China), sodium hydroxide (NaOH, 96%, Sinopharm Chemical Reagent Co. Ltd., Shanghai, China) and nitric acid (HNO_3, Sinopharm Chemical Reagent Co. Ltd., Shanghai, China). All chemical reagents are used as received without further purification.

2.2. Preparation procedure

The $RE(NO_3)_3$ (RE=Gd and Dy) solutions were prepared via dissolving Gd_2O_3 and Dy_2O_3 in hot nitric acid. The mother salt solution was prepared by $RE(NO_3)_3$ and $Na_2WO_4{\cdot}2H_2O$ according to the chemical formula of $(Gd_{1-x}Dy_x)_2(WO_4)_3$

After the above process is completed, a certain proportion of $Na_2WO_4{\cdot}2H_2O$ white particles dissolved in 50 ml water, then take the appropriate amount of nitrate solution dissolved in 20 ml water, respectively, placed in a collector type thermostatic magnetic stirrer, stirring about 5 min; When the two raw materials are fully dissolved and stirred in deionized water, the resulting nitrate aqueous solution is uniformly dropped into the sodium tungstate solution and treated at the end of the titration for 30 min, add NaOH solution to the mixture and adjust the pH until pH=7, The resulting reaction solution is then moved to a stainless steel autoclave in the capacity of 100 ml; The reaction kettle is placed in the oven and the oven is set at a temperature of 120℃, and the reaction time is 24 h. When the reaction is finished, the reaction kettle is cooled to room temperature and the hydrothermal product is removed; The obtained hydrothermal product is washed repeatedly by deionized water and once cleaned by anhydrous ethanol, and the product is dispersed into alcohol and dried in a drying box (80℃, dried 6 h) to obtain precursor; Finally, the precursor was calcined in an air atmosphere at high temperature (900℃ 2 h), and finally the target phosphor was obtained

2.3. Characterization

The XRD patterns were collected at room temperature by diffractometer (Model D8 ADVANCE, BRUKER Co., Germany) using nickel-filtered CuK_α radiation in the 2θ range 10-70° at a scan rate of 4.0° 2θ/min. The morphologies of products were observed by the FE-SEM with an acceleration voltage of 10 kV (Model QUANTA FEG 250, FEI Co., America). The PL/PLE spectra of the $(Gd_{1-x}Dy_x)_2(WO_4)_3$ phosphors were studied by a fluorescence spectrophotometer (FP-6500, JASCO, Tokyo, Japan) equipped with a Φ60-mm intergating sphere (Model ISF-513, JASCO, Tokyo, Japan) and a 150-W Xe-lamp as the excitation source.

3. Results and discussion

The XRD patterns of the $(Gd_{1-x}Dy_x)_2(WO_4)_3$ phosphors calcined at the same temperature 900℃ with different Dy^{3+} contents (x=0.01, 0.05 and 0.10) are shown in Fig. 1. It is well known that the pure phase is beneficial to the luminescent properties of phosphors. As shown in Fig. 1, all the Dy^{3+}-free samples can be well indexed to $Gd_2(WO_4)_3$ with the bottom centered monoclinic structure (space group: C_2/c, JCPDS: no.23-1076) [12]. No additional diffraction peaks were observed on the XRD spectra indicating that the pure phase $(Gd_{1-x}Dy_x)_2(WO_4)_3$ has been formed and Dy^{3+} doping does not change the crystal structure.

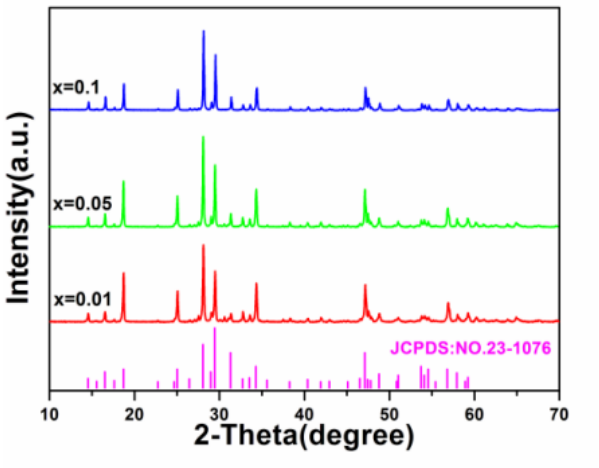

Figure 1. XRD spectra of $(Gd_{1-x}Dy_x)_2(WO_4)_3$ calcined 900 °C at as function of Dy^{3+} content (x value)

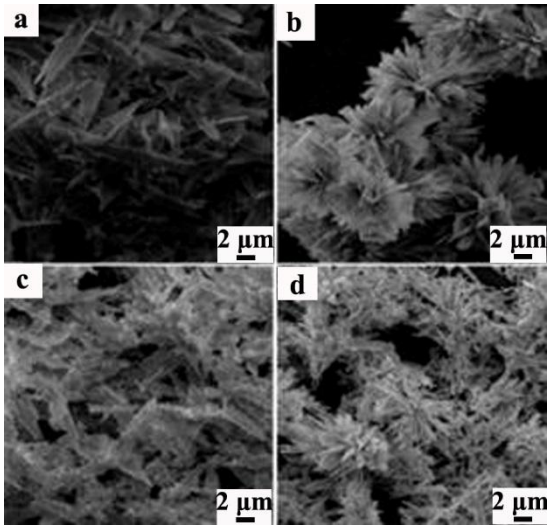

Figure 2. FE-SEM of the $(Gd_{1-x}Dy_x)_2(WO_4)_3$ precursors, x=0.01 (a), x=0.10 (b), and the precursors calcined at 900 °C, x=0.01 (c), x=0.1 (d)

Fig. 2 shows FE-SEM micrographs of $Gd_2(WO_4)_3$ with different Dy^{3+} content. From which it can be seen that the particle shape of samples does not change significantly with the Dy^{3+} incorporation, and all the precursors show needle-like appearance. The products with good dispersion calcined at 900℃ maintain the morphology of precursor.

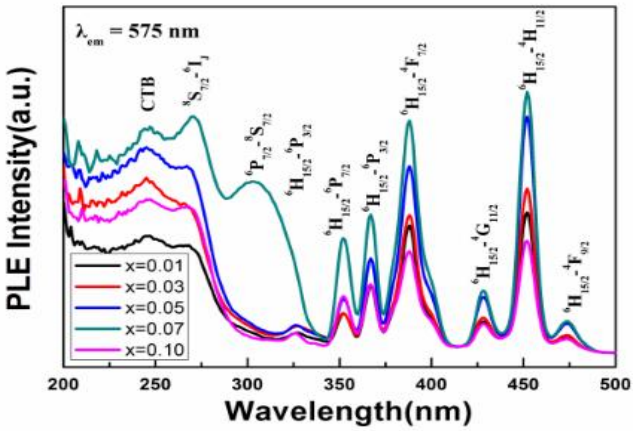

Figure 3. PLE spectra of the $(Gd_{1-x}Dy_x)_2(WO_4)_3$ phosphors calcined at 900 °C. The PLE spectra were taken by monitoring the 575 nm emission

Fig. 3 shows the excitation spectra of Dy^{3+} doped $Gd_2(WO_4)_3$ phosphor as a function of Dy^{3+} content. The PLE spectra all mainly are composed of five excitation bands and the excitation intensity of the 452 nm (Dy^{3+}: $^6H_{15/2} \rightarrow {}^4H_{11/2}$) wavelength is the strongest. The excitation peak at 245 nm

originates from the charge transfer band transition of W-O proving direct evidence of $WO_4^{2-} \rightarrow Dy^{3+}$ energy transfer. The $^8S_{7/2} \rightarrow {}^6I_J$ transition of Gd^{3+} appeared at ~270 nm [13-14] indicating the efficient energy transfer from Gd^{3+} to Dy^{3+}. As shown in Fig. 3, the other bands observed in the longer wavelength region at ~352, ~366, ~386, ~427 and ~470 nm are corresponded to the $^6H_{15/2} \rightarrow {}^6P_{7/2}$, $^6H_{15/2} \rightarrow {}^6P_{3/2}$, $^6H_{15/2} \rightarrow {}^4F_{7/2}$, $^6H_{15/2} \rightarrow {}^4G_{11/2}$ and $^6H_{15/2} \rightarrow {}^4F_{9/2}$ transitions of Dy^{3+}, respectively.

Fig. 4 shows the PL properties obtained under UV excitation at 452 nm of the $(Gd_{1-x}Dy_x)_2(WO_4)_3$ phosphors calcined at 900℃. The PL spectra for all the samples with different Dy^{3+} concentrations include three emission banks at ~480 nm (blue), ~575 nm (yellow, the strongest) and ~663 nm (red), corresponding to the $^4F_{9/2} \rightarrow {}^6H_{15/2}$, $^4F_{9/2} \rightarrow {}^6H_{13/2}$ and $^4F_{9/2} \rightarrow {}^6F_{11/2}$ transitions of Dy^{3+}, respectively [15]. Further observation is that the yellow emission is much stronger than the blue one in each case, and the integrated intensities of the yellow to blue emission bands have ratios of ~3.91, 4.13, 4.18, 4.30 and 4.33 for the different Dy^{3+} contents studied in this work. The reason is that the Judd-Ofelt parity law [16, 17] predicts that the magnetic dipole transition of $^4F_{9/2} \rightarrow {}^6H_{15/2}$ is allowed while the electric dipole transition of $^4F_{9/2} \rightarrow {}^6H_{13/2}$ is forbidden, the electric dipole transition is permitted only when the Dy^{3+} ions occupy a low symmetry site without an inversion center. $Gd_2(WO_4)_3$ is a bottom centered monoclinic structure,, the Gd^{3+} mainly occupies the low symmetry site without an inversion center [18]. The Dy^{3+} ions are expected to partially substitute for Gd^{3+}, and thus the emission spectra are thus dominated by the $^4F_{9/2} \rightarrow {}^6H_{13/2}$ forced electric dipole transition at 575 nm rather than $^4F_{9/2} \rightarrow {}^6H_{15/2}$ magnetic dipole transition at 480 nm. The Dy^{3+} addition does not alter the emission peak position and shape significantly, but the intensity varied. The inset in Fig. 4 shows intensity of the 575 nm emission (λ_{ex}=452 nm) plotted against Dy^{3+}concentration. It is clearly seen that the intensity steadily improves with increasing Dy^{3+} doping up to 7.0 at% (x=0.07) and then rapidly deteriorates owing to concentration quenching. The optimal Dy^{3+} content is thus determined to be 7.0 at% (x=0.07).

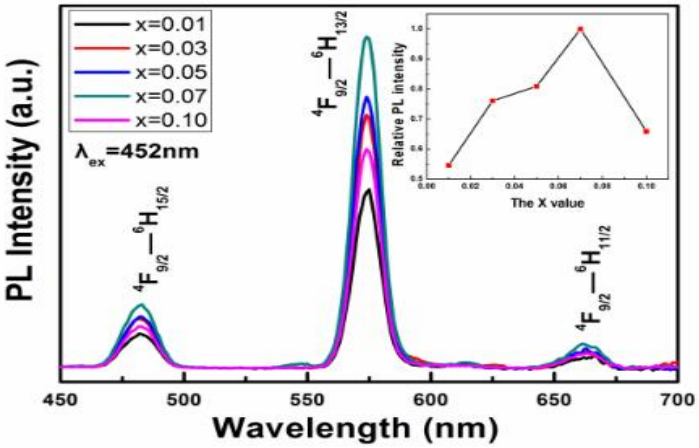

Figure 4. PL spectra of the $(Gd_{1-x}Dy_x)_2(WO_4)_3$ phosphors calcined at 900 °C. The PL spectra were measured under UV excitation at 452 nm. The inset is the relative intensity of the 575 nm emission, normalized to that of the $(Gd_{0.93}Dy_{0.07})_2(WO_4)_3$ phosphors, as a function of the Dy^{3+} content

The interaction type of luminescence quenching in solid phosphors can be concluded by analyzing the constants according to the following equation [19]:

$$\log(I/c) = (-s/d)\log c + \log f \quad (1)$$

where I is the emission intensity, c the activator concentration, d the sample dimension (d=3 for regular sample), f is a constant, and s is the index of electric multipole. The s values of 6, 8, and 10 represent the dipole-dipole, dipole-quadrupole, and quadrupole-quadrupole electric interactions, respectively, whereas s=3 corresponds to exchange interaction. The log(I/c)-log(c) plot of the 575 nm emission is given in Fig. 5. The slope (-$s/3$) was determined to be -0.933 yielding an s value of ~ 2.8

for the Dy^{3+} doped $Gd_2(WO_4)_3$ systems. This indicates that the concentration quenching is mainly due to the energy transfer between Dy^{3+}-Dy^{3+} [20].

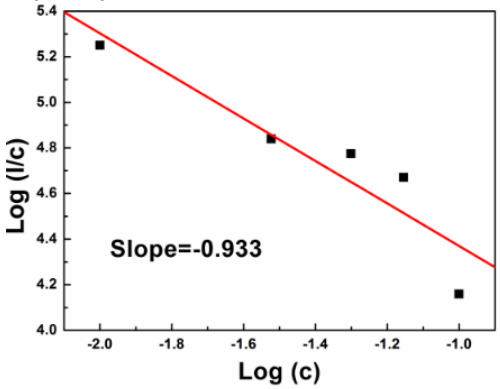

Figure 5. The relationship between log(*I*/*c*) and log(*c*) for the $(Gd_{1-x}Dy_x)_2(WO_4)_3$ samples calcined at 900 °C

Fig. 6 shows the decay kinetics for the 575 nm emission of $(Gd_{0.93}Dy_{0.07})_2(WO_4)_3$ calcined at 900 ℃ for 2 h. The decay curve can be fitted via the equation:

$$I = A\exp\left(-t/\tau_R\right) + B \tag{2}$$

where *I* is the relative fluorescence intensity, t is the decay time, τ_R is the fluorescence lifetime. *A* and *B* are constants [21]. The fitting results are A=7.19±0.07, B=-0.03±0.07, τ_R=0.55±0.004 ms. The inst (a) in Fig. 6 displays the lifetime value against the Dy^{3+} concentration. The lifetime shortens from 0.56 ms to 0.48 ms when the content of Dy^{3+} increases from *x*=0.01 to *x*=0.10. The shortened lifetime can be explained as follows: when the Dy^{3+} content is low, the distance among the Dy^{3+} ions is relatively long and the interaction among luminescent centers can be neglected. A higher Dy^{3+} concentration would lead to the formation of a resonant energy transfer net, which can act as an additional channel to the nonradiative centers of surface and therefore shorten the lifetime. The inset (b) in Fig.6 shows the lifetime of the $(Gd_{0.93}Dy_{0.07})_2(WO_4)_3$ at the temperature of 423 K. The fitting results are *A*=1.73±8.45, *B*=-0.03±0.27, τ_R=0.45±0.001 ms. The used temperature does not affect the fluorescence lifetime appreciably, and the lifetime in the temperature range 298-573 K was similar to be ~0.5±0.05 ms.

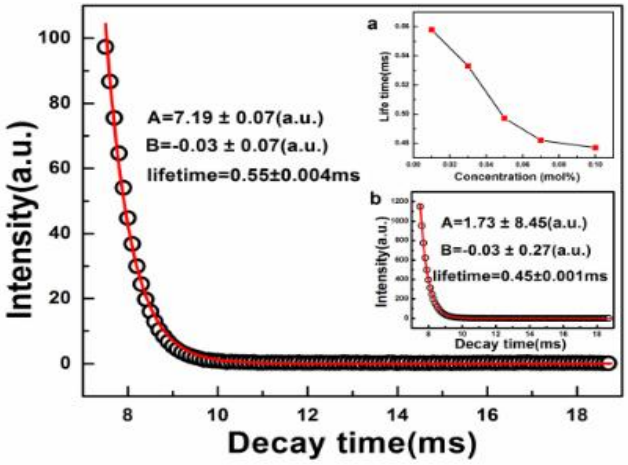

Figure 6. Fluorescence decay curve for the 575 nm emission of $(Gd_{0.93}Dy_{0.07})_2(WO_4)_3$ phosphors calcined at 900 °C for 2 h. The inset (a) in the figure is the lifetime values as function of Dy^{3+} content, (b) is the fluorescence decay curve for the 575 nm emission of $(Gd_{0.93}Dy_{0.07})_2(WO_4)_3$ at used temperature of 423 K

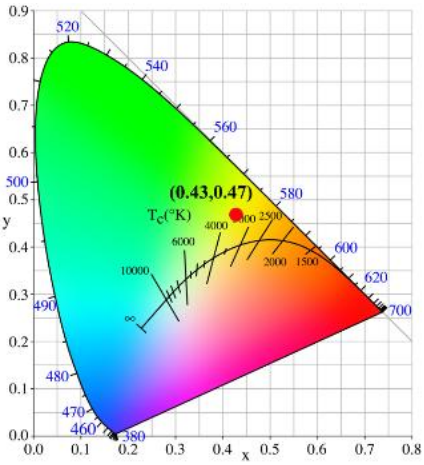

Figure 7. CIE chromaticity diagram for the $(Gd_{0.93}Dy_{0.07})_2(WO_4)_3$ system under 452 nm excitation

Moreover, the color chromaticity coordinates of phosphor has been calculated by using the CIE 1931 color matching functions, and the result was shown in Fig. 7. Fig. 7 shows the CIE chromaticity diagram of $(Gd_{0.93}Dy_{0.07})_2(WO_4)_3$ phosphor under 452 nm light excitation. The CIE chromaticity coordinate of sample $(Gd_{0.93}Dy_{0.07})_2(WO_4)_3$ is determined to be (0.43, 0.47), indicating that the samples emit a vivid yellow color. The corresponding color temperature was calculated to be ~3550 K according to the following formulas [22]:

$$T = -437n^3 + 3601n^2 - 6861n + 5514.31 \quad (3)$$

$$n = (x - 0.332)/(y - 0.1858) \quad (4)$$

It should be noted that all the samples studied in this work have almost identical CIE chromaticity coordinate and color temperature of (0.43±0.02, 0.47±0.02), and ~3550 K, respectively.

The CIE coordinate (*x, y*) of $(Gd_{0.93}Dy_{0.07})_2(WO_4)_3$ is (0.4300, 0.4700). The dominant wavelength of $(Gd_{0.93}Dy_{0.07})_2(WO_4)_3$ is determined to be 575 nm, and we can obtain the (x_d, y_d) chromaticity coordinate of $(Gd_{0.93}Dy_{0.07})_2(WO_4)_3$ is (0.5096, 0.4904). By substituting the coordinates of (*x, y*), (x_i, y_i), and (x_d, y_d) in equation (6), the color purities of $(Gd_{0.93}Dy_{0.07})_2(WO_4)_3$ is calculated to be 71%. This result indicates that $(Gd_{1-x}Dy_x)_2(WO_4)_3$ phosphor is a deep yellow phosphor and features higher color purity.

4. Conclusions

In the experiment, the $Gd_2(WO_4)_3$ doped Dy^{3+} phosphors were successfully obtained via hydrothermal method. The phase-pure $(Gd_{1-x}Dy_x)_2(WO_4)_3$ with good dispersion and uniform particle size formed at 900 ℃. The $(Gd_{1-x}Dy_x)_2(WO_4)_3$ phosphors with needle-like feature exhibit strong yellow emission at 575 nm ($^4F_{9/2} \rightarrow {}^6H_{13/2}$ transition of Dy^{3+}) under UV excitation into the $^6H_{15/2} \rightarrow {}^4H_{11/2}$ of Dy^{3+} at ~452 nm. The currence of charge transfer band of W-O and $^8S_{7/2} \rightarrow {}^6I_J$ transition of Gd^{3+} provide the direct evidence of the $WO_4^{2-} \rightarrow Dy^{3+}$ and $Gd^{3+} \rightarrow Dy^{3+}$ energy transfer. The quenching concentration of $(Gd_{1-x}Dy_x)_2(WO_4)_3$ phosphors was determined to be 7 at% (x=0.07) and the luminescence quenching is dominated by exchange interactions resulting from the energy transfer among Dy^{3+} ions. All the $(Gd_{1-x}Dy_x)_2(WO_4)_3$ phosphors have the similar CIE chromaticity coordinates, and color temperatures of (~0.43±0.02, ~0.47±0.02), and ~3550 K, respectively. By analyzing the fluorescence decay kinetics of $Gd_2(WO_4)_3$:Dy^{3+} phosphor, it is found that the fluorescence lifetime of best $(Gd_{0.93}Dy_{0.07})_2(WO_4)_3$ sample was determined to be 0.55±0.004 ms, and the lifetime shortens with the increase of Dy^{3+} concentration while changes little with the temperature increasing.

5. Acknowledgments

This work was supported in part by the National Natural Science Foundation of China (No. 51402125, and 51602042), China Postdoctoral Science Foundation (No. 2017M612175), the Special Fund for the Postdoctoral Innovation Project in Shandong Province (No. 201603061), the Research Fund for the Doctoral Program of University of Jinan (No. XBS1447), the Natural Science Foundation of University of Jinan (No. XKY1515), the Science Foundation for Post Doctorate Research from the University of Jinan (172335).

References

[1] Brixner L H, Sleight A W. Crystal growth and precision lattice constants of some $Ln_2(WO_4)^{3-}$ type rare earth tungstates. Mater. Res. Bull., 1973, 8(10):1269.
[2] Keve E T, Abrahams S C, Bernstein J L. Ferroelectric paramagnetic beta-$Gd_2(MoO_4)_3$ crystal structure of the transition-metal molybdates and tungstates. J. Chem. Phys., 1971, 54(7): 3185.
[3] Nassau K, Levinstein H J, Loiacono G M. A comprehensive study of trivalent tungstates and molybdates of the type $L_2(MO_4)_3$. J. Phys. Chem. Solids, 1965, 26: 1805.
[4] Liu Z, Meng Q, Liu H, Yao C, Meng Q, Liu W, Wang W. Energy transfer and electron-phonon coupling properties in $Gd_2(WO_4)_3$:Eu phosphor. Opt. Mater., 2013, 36(2): 384.

[5] Zeng Y, Li Z, Wang L, Xiong Y. Controlled synthesis of $Gd_2(WO_4)_3$ microstructures and their tunable photoluminescent properties after Eu^{3+}/Tb^{3+} doping. CrystEngComm, 2012, 14(20): 7043.
[6] Kodaira C A, Brito H F, Felinto M C F C. Luminescence investigation of Eu^{3+} ion in the $RE_2(WO_4)_3$ matrix (RE=La and Gd) produced using the Pechini method. J. Solid State Chem., 2003, 171(1): 401.
[7] Li J K, Teng X, Wang W Z, Zhao W L, Liu Z M. Investigation on the preparation and luminescence property of $(Gd_{1-x}Dy_x)_2O_3$ (x = 0.01-0.10) spherical phosphors. Ceram. Int., 2017, 43: 10166.
[8] Li J G, Sakka Y. Recent progress in advanced optical materials based on gadolinium aluminate garnet ($Gd_3Al_5O_{12}$). Sci. Technol. Adv. Mat., 2015, 16(1): 14902.
[9] Wang W, Li J K, Duan G, Zhao W, Cao B, Liu Z. Morphology/size effect on the luminescence properties of the $[(Y_xGd_{1-x}0.98Dy_{0.02}]_2O_3$ phosphor with enhanced yellow emission. J. Lumin., 2017, 192: 1056.
[10] Wang J, Zhang Z J, Zhao J T, Chen H H, Yang X X, Tao Y, Huang Y. Luminescent metastable Y_2WO_6:Ln^{3+} (Ln=Eu, Er, Sm, and Dy) microspheres with controllable morphology via self-assembly. J. Mater. Chem., 2010, 20(48): 10894.
[11] Ding B, Han C, Zheng L, Zhang J, Wang R, Tang Z. Tuning oxygen vacancy photoluminescence in monoclinic Y_2WO_6 by selectively ℃cupying yttrium sites using lanthanum. Sci. Rep-UK, 2015, 5: 9443.
[12] Lu H, Hao H, Gao Y, Li D, Guang G, Song Y, Wang Y, Zhang X. Optical sensing of temperature based on non-thermally coupled levels and upconverted white light emission of a $Gd_2(WO_4)_3$ phosphor co-doped with in Ho (III), Tm (III), and Yb (III). Micr℃him. Acta, 2017, 184(2): 641.
[13] Mahlik S, Lazarowska A, Grobelna B, Grinberg M. Luminescence of Gd2(WO4)3:Ln^{3+} at ambient and high hydrostatic pressure. J. Phys-Condens. Mat., 2012, 24(48): 485501.
[14] Kim J. The role of auxiliary alkali metal ions on scheelite structure double molybdate and tungstate phosphors. Inorg. Chem., 2017, 56(14).
[15] Li J K, Li J G, Liu S H, Sun X D, Sakka Y. Greatly enhanced Dy^{3+} emission via efficient energy transfer in gadolinium aluminate garnet ($Gd_3Al_5O_{12}$) stabilized with Lu^{3+}. J. Mater. Chem. C, 2013, 1(45): 7614.
[16] Kaczmarek A M, Hecke K V, Deun R V. Enhanced luminescence in Ln^{3+}-doped Y_2WO_6 (Sm, Eu, Dy) 3D microstructures through Gd^{3+} codoping. Inorg. Chem., 2014, 53(18): 9498.
[17] Sun J, Yu T, Li X, Zhang J, Cheng L, Zhong H, Tian Y, Hua R, Chen B. Co-precipitation synthesis, structural and morphological characterization, and luminescence properties of Dy^{3+} doped nanocrystal $Gd_2(WO_4)_3$ and Gd_2WO_6 phosphors. J. Phys. Chem. Solids, 2012, 73(3): 465.
[18] Li J K, Li J G, Zhang Z, Wu X, Liu S, Li X, Sun X, Sakka Y. Gadolinium aluminate garnet ($Gd_3Al_5O_{12}$): crystal structure stabilization via lutetium doping and properties of the $(Gd_{1-x}Lu_x)_3Al_5O_{12}$ solid solutions (x=0–0.5). J. Am. Ceram. Soc. 2012, 95(3): 931.
[19] Li J K, Li J G, Li X, Sun X. Tb^{3+}/Eu^{3+} codoping of Lu^{3+}-stabilized $Gd_3Al_5O_{12}$ for tunable photoluminescence via efficient energy transfer. J. Alloy. Compound., 2016, 670: 161.
[20] Shukla R, Ningthoujam R S, Tyagi A K, Vatsa R K. Luminescence properties of Dy^{3+} doped Gd_2O_3 nanoparticles prepared by glycine route: annealing effect. Int. J. Nanotechnol., 2010, 7: 843.
[21] Li J, Wu Z, Sun X, Zhang X, Dai R, Zuo J, Zhao Z. Controlled hydrothermal synthesis and luminescent properties of Y_2WO_6:Eu^{3+} nanophosphors for light-emitting diodes. J. Mater. Sci., 2017, 52(6): 3110.
[22] Mccamy C S. Correlated color temperature as an explicit function of chromaticity coordinates. Color Res. Appl., 1992, 17(2): 142.